

Magnetic effects of alteration in mineral systems

David A. Clark^[1]

1. CSIRO Manufacturing, Superconducting Systems and Devices Group, & CSIRO Mineral Resources

ABSTRACT

Magnetic anomaly patterns can be used as a tool for mapping lithology, metamorphic zones and hydrothermal alteration systems, as well as identifying structures that may control passage of magmas or hydrothermal fluids associated with mineralization. Reliable geological interpretation of mineralized systems requires an understanding of the magmatic, metamorphic and hydrothermal processes that create, alter and destroy magnetic minerals in rocks. Predictive magnetic exploration models for porphyry copper and iron oxide copper-gold (IOCG) deposits can be derived from standard geological models by integrating magnetic petrological principles with petrophysical data, deposit descriptions, and modelling of observed magnetic signatures of these deposits. Even within a particular geological province, the magnetic signatures of similar deposits may differ substantially, due to differences in the local geological setting. Searching for “look-alike” signatures of a known deposit is likely to be unrewarding unless pertinent geological factors are taken into account. These factors include the tectonic setting and magma type, composition and disposition of host rocks, depth of emplacement and post-emplacement erosion level, depth of burial beneath younger cover, post-emplacement faulting and tilting, remanence effects contingent on ages of intrusion and alteration, and metamorphism. Because the effects of these factors on magnetic signatures are reasonably well understood, theoretical magnetic signatures appropriate for the local geological environment can qualitatively guide exploration and make semiquantitative predictions of anomaly amplitudes and patterns. The predictive models also allow detectability of deposit signatures to be assessed, for example when deposits are buried beneath a considerable thickness of nonmagnetic overburden, are covered by highly magnetic heterogeneous volcanic rocks, or there is a strong regional magnetic gradient. This paper reviews the effects of hydrothermal alteration on magnetic properties and magnetic signatures of porphyry copper and iron oxide copper-gold systems and presents examples of predictive magnetic exploration models, and their predicted signatures, in various geological circumstances. This paper also presents a list of criteria for interpreting magnetic surveys and magnetic petrophysical data, which are aimed at guiding exploration for porphyry, epithermal and IOCG deposits.

INTRODUCTION

Magnetic surveys rapidly provide cost-effective information on the magnetization distribution of the Earth's crust, at all scales from local to global. In particular, aeromagnetics is the most widely used geophysical method in hard rock mineral exploration from prospect to province scales. The anomaly patterns revealed by such surveys can be used as a tool for mapping lithology, metamorphic zonation and hydrothermal alteration assemblages, as well as identifying structures that may control passage of magmas or hydrothermal fluids associated with mineralization. Magnetic anomalies can also provide a direct indication of certain types of ore deposit or mineralized system. A non-exhaustive list includes Kiruna-type magnetite-apatite deposits, iron oxide copper-gold (IOCG) deposits, gold-rich porphyry copper deposits, magnetite and/or pyrrhotite-bearing volcanogenic massive sulfide deposits, pyrrhotite-rich massive nickel sulfide deposits, and diamondiferous kimberlite pipes.

Magnetic signatures of mineralization are not always associated with strongly magnetic sources, but can be indicated by zones of anomalously weak magnetization. For example, epithermal precious metal deposits hosted by mafic or intermediate volcanic rocks are often associated with smooth magnetic lows, produced by magnetite-destructive alteration, surrounded by the characteristic short wavelength, large

amplitude magnetic anomaly patterns of the heterogeneously magnetized unaltered volcanics.

Readers are referred to Clark (1997) for a review of magnetic petrophysics and principles of magnetic petrology. Clark (1999) discussed the magnetic petrology of igneous intrusions and discussed implications for exploration. Clark (2014) published a comprehensive review of magnetic effects of alteration in porphyry copper and iron-oxide copper-gold (IOCG) systems. Useful case histories of magnetic signatures of hydrothermal alteration effects include Criss and Champion (1984), Criss et al. (1985), Lapointe et al. (1986), Allis (1990), Irvine and Smith (1990), Finn et al. (2001, 2002, 2007) and Airo (2002).

MAGNETIC PETROLOGY OF IGNEOUS INTRUSIONS ASSOCIATED WITH MINERALIZATION

Significance of oxidation state

Igneous rocks associated with mineralized systems can be classified into four groups on the basis of the oxidation state: strongly reduced, reduced, oxidized, or strongly oxidized (Champion and Heinemann, 1994). These categories can be determined on the basis of chemistry, if ferrous and ferric iron contents are known, as shown in Figure 1, or mineralogy.

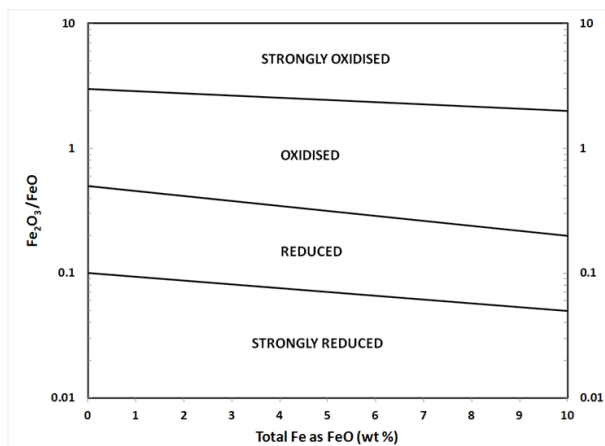


Figure 1. Classification of oxidation state of igneous rocks on the basis of $\text{Fe}_2\text{O}_3/\text{FeO}$ (both expressed as weight per cent). Fields for strongly oxidized, oxidized, reduced and strongly reduced rocks are taken from Champion and Heinemann (1994), following Ishihara et al. (1979) and Blevin and Chappell (1992). Strongly oxidized igneous rocks contain magmatic magnetite + primary sphene \pm hematite. Oxidized rocks contain (titano)magnetite \pm ilmenite with high Fe^{3+} or high Mn. Reduced igneous rocks contain ilmenite without magnetite and strongly reduced igneous rocks contain ilmenite, with low Fe^{3+} and Mn, plus pyrrhotite, with no magnetite.

Significant differences in magnetic susceptibility, at equivalent degrees of differentiation, are found for mantle-derived (M-type) intrusions, found typically in island arcs, and I-type granitoids in continental arcs. Intrusions associated with gold-rich porphyry copper deposits are more oxidized than those associated with gold-poor porphyry copper deposits, and accordingly contain more abundant igneous (titano)magnetite and produce greater quantities of hydrothermal magnetite during early potassic alteration. Although primary magmatic hematite can also occur in association with magnetite, magmas that are sufficiently oxidized to precipitate abundant hematite, with little or no magnetite, are unusual. An empirical association between Au-rich (> 0.4 g/t) porphyry copper deposits and abundant magnetite in the potassic core has been documented by Sillitoe (1979, 1990, 1993, 1996) and confirmed by many other workers. The corresponding magnetic signatures also differ profoundly, with more prominent anomalies associated with gold-rich porphyry copper deposits than with gold-poor deposits. Clark (1999, 2014) has extensively reviewed the association between oxidation state and metallogeny.

Studemeister (1983) pointed out that the redox state of iron in rocks is a useful indicator of hydrothermal alteration. Large volumes of fluid or high concentrations of exotic reactants, such as hydrogen or oxygen, are required to shift $\text{Fe}^{3+}/\text{Fe}^{2+}$ ratios. When reactions associated with large water/rock ratios occur, the change in redox state of the rocks produces large changes in magnetic properties due to creation or destruction of ferromagnetic minerals.

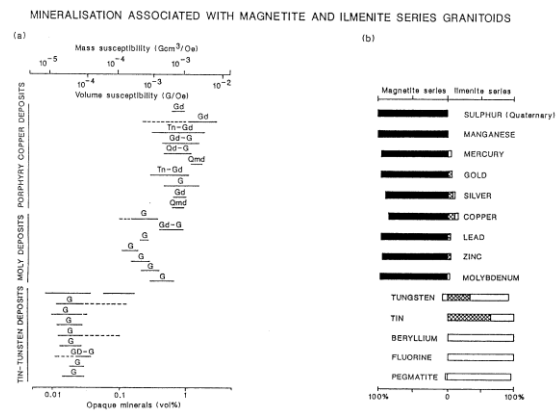


Figure 2. Range of CGS mass and volume susceptibilities and opaque mineral contents for granitoids associated with porphyry Cu, granitoid-related Mo deposits and granitoid-related Sn-W deposits (Gd = granodiorite, Tn = tonalite, G = granite, Qmd = quartz monzodiorite). (b) Proportions of mineral deposits, of a variety of commodities, that occur within magnetite-series and ilmenite-series granitoid belts. Hatched regions represent WFM magnetite-series granitoids. The mineral deposits are inferred to be genetically related to granitoids or to their associated volcanics. Pegmatite refers to stanniferous pegmatite deposits. SI volume susceptibility = CGS volume susceptibility (G/Oe) $\times 4\pi$; mass susceptibility = volume susceptibility/density (after Ishihara, 1981).

Influence of host rocks

The nature of the country rock is crucial in the case of magmatic-hydrothermal skarn deposits, which develop in carbonate rocks that have been metamorphosed and metasomatized by the mineralizing intrusion. In most cases emplacement of the intrusion into non-carbonate rocks would not have resulted in economic mineralization. The review of Einaudi *et al.* (1981) contains much useful information relevant to magnetic petrology of skarn deposits. Magnetite contents of magnesium skarns developed in dolomite are generally higher than those of calcic skarns developed in limestone, because Fe-rich calc-silicates are not stable in a high-Mg system. However both island arc-type calcic skarns (associated with gabbros and diorites in volcano-sedimentary sequences) and Cordilleran-type magnesian skarns (associated with quartz monzonites or granodiorites intruding dolomites) have been mined for magnetite. Such deposits are evidently associated with very large magnetic anomalies.

Cu skarns (mostly associated with epizonal quartz monzonite and granodiorite stocks in continental settings) are associated with oxidized assemblages, including magnetite + hematite, with the less common magnesian skarns exhibiting higher magnetite and lower sulfide contents than calcic skarns. Tungsten-bearing skarns (associated with mesozonal calc-alkaline quartz monzonite to granodiorite intrusions) have a more reduced calc-silicate and opaque mineralogy than Cu-skarns, but typically contain minor magnetite and/or pyrrhotite and would therefore be expected to exhibit a relatively weak, but nevertheless detectable, magnetic signature in most cases. Calcic Zn-Pb skarn deposits associated with granodioritic to granitic magmatism and Mo skarns

associated with felsic granites appear to contain relatively little magnetite. Sn skarns are associated with reduced ilmenite-series granites and have relatively low sulfide contents. The skarns themselves contain magnetite \pm pyrrhotite and exhibit a substantially larger susceptibility than the paramagnetic granite and unaltered host rocks. Massive sulfide replacement tin orebodies in dolomite (e.g. Renison and Cleveland deposits, Tasmania) are rich in monoclinic pyrrhotite and have high susceptibilities, with substantial remanent magnetization. This type of orebody may represent the low temperature distal analogue of magnesian Sn skarns.

Webster (1984) analyzed magnetic patterns over a number of granitoids associated with tin mineralization in the Lachlan Fold Belt and contrasted these with unmineralized and Cu-Mo-W mineralized granitoids. The characteristic magnetic signature of granitoid-associated tin mineralization is: a granitoid with low magnetic relief, surrounded by a more magnetic aureole, with significant magnetic anomalies associated with the mineralization.

Wyborn and Heinrich (1993a,b) and Wyborn and Stuart-Smith (1993) have suggested that particular host rocks favour deposition of Au mineralization from oxidized fluids that emanate from felsic granitoids and move up to 5 km from the granitoid contact. Graphite-, sulfide- and magnetite-bearing lithologies are capable of reducing the fluids and depositing Au and Cu, whereas Pb and Zn are preferentially deposited in carbonate rocks. Au-only mineralization will preferentially be deposited within graphite-bearing but magnetite- and sulfide-poor rocks, whereas magnetite and or iron sulfide-rich rocks tend to precipitate Cu and Au together. These relationships appear to have been observed in the eastern Mount Isa Inlier and the Pine Creek Inlier. Thus a rock unit that is strongly magnetic, indicative of high magnetite content, may be a favorable site for deposition of Au-Cu mineralization sourced from a nearby granitoid.

Alteration in porphyry copper systems

The types of hydrothermal alteration that are important in porphyry copper systems and their magnetic effects are summarized in Table 1. The magnetic mineralogy of the altered rock depends on the abundance and composition of primary magnetic minerals, their stability under the prevailing hydrothermal conditions, and on the ability of the protolith to create secondary magnetic minerals during reaction of the hydrothermal fluid with the pre-existing mineralogy. For example, mafic wall rocks have greater capacity to form secondary magnetite during potassic alteration than do relatively iron-poor felsic rocks.

Alteration zoning patterns within carbonate wall rocks, which are highly reactive and acid-neutralising, differ profoundly from those in silicate wall rocks. Porphyry systems emplaced into carbonate host rocks develop mineralogically and magnetically zoned skarns. Table 2 lists magnetic properties of skarns inferred from these descriptions and Table 3 gives estimated zonation of magnetic susceptibility inferred from reported modal mineralogy for a typical copper skarn.

Table 4 summarizes the differences between alteration assemblages developed around porphyry copper deposits in mafic, felsic and carbonate host rocks.

Intense epithermal-style alteration, whether low- or high-sulfidation, is invariably magnetite-destructive. The magnetic signature is strongly dependent on the host rocks. Epithermal alteration systems hosted by magnetic volcanic rocks are characterized by smooth, flat magnetic low zones within the overall busy magnetic texture. Similar systems within non-magnetic sedimentary rocks have negligible magnetic expression. High sulfidation systems may have a diffuse intrusion + alteration high due to a deeper porphyry system within a few hundred meters to a few kilometres of the deposit. This may be more prominent if post-formation faulting has brought the intrusion closer to the surface, or the porphyry and epithermal systems are telescoped by rapid uplift during formation.

PREDICTIVE MAGNETIC EXPLORATION MODELS

Clark *et al.* (2004) developed the concept of predictive magnetic exploration models for porphyry copper, volcanic-hosted epithermal and IOCG deposits. Purucker and Clark (2011) presented some examples of these models. The predictive models are based on magnetic petrological principles, standard geological models, deposit descriptions, magnetic petrophysical data from deposits and observed magnetic signatures. They are designed to predict what the magnetic signatures of these deposits should look like in a variety of different geological settings, by taking into account the geological factors that control the magnetic signatures. These factors include the tectonic setting and magma type, composition and disposition of host rocks, depth of emplacement and post-emplacement erosion level, depth of burial beneath younger cover, post-emplacement faulting and tilting, remanence effects contingent on ages of intrusion and alteration, and metamorphism. Even within a particular geological province, these factors may vary greatly and the magnetic signatures of similar deposits may therefore differ substantially. Searching for “look-alike” signatures of a known deposit is likely to be unrewarding unless the local geological setting is taken into account.

Oxidized gold-rich porphyry copper model

Phyllic alteration, argillic alteration and intense propylitic alteration associated with porphyry intrusions tend to destroy magnetite within the intrusion and in surrounding rocks. Weak to moderate, but pervasive, propylitic alteration may leave most of the magnetite in host rocks relatively unaffected. On the other hand, the potassic alteration zone associated with oxidized, magnetic felsic intrusions is often magnetite-rich. This is commonly observed for Au-rich porphyry copper systems (Sillitoe, 1979). Clark *et al.* (1992) presented a theoretical magnetic signature of an idealized gold-rich porphyry copper deposit, based on the Sillitoe (1979) model and magnetic petrological concepts. This model underwent further development, incorporating petrophysical, geophysical and geological data from well-characterized gold-rich porphyry copper deposits (Clark *et al.*, 2004; Clark, 2014).

Figure 3 shows the geometry of an end-member gold-rich porphyry copper model, with maximal development of magnetite in the potassic zone, hosted by intermediate-mafic oxidized igneous rocks (nominally “andesite”). In this case there has been insufficient erosion to expose the deposit. The top of the mineralization lies 500 m below the surface and the only sign of the mineralized system at the surface is a patch of propylitic alteration that could easily be overlooked or, if observed, assumed to be of little significance. Table 5 lists the dimensions and susceptibilities incorporated into this model.

The inner potassic zone is strongly mineralized and magnetite-rich. It is surrounded by an outer potassic zone that contains less abundant, but still significant, magnetite. The inner potassic zone represents relatively intense development of quartz-magnetite-K feldspar veins, whereas the outer potassic zone corresponds to biotite-K feldspar-quartz-magnetite alteration. A shell of magnetite-destructive phyllic alteration with very low susceptibility envelops the potassic zones. At upper levels this alteration may grade into intermediate argillic and shallow advanced argillic alteration, but the magnetic properties are equivalent for these alteration types and a single shell is sufficient to model the effects. The phyllic zone is surrounded by a zone of intense propylitic alteration, which is partially magnetite-destructive, which passes out into weak propylitic alteration and then into unaltered andesite. This model is largely based on the Bajo de la Alumbrera deposit in Argentina, which has a spectacular “archery target” magnetic signature (Figure 4).

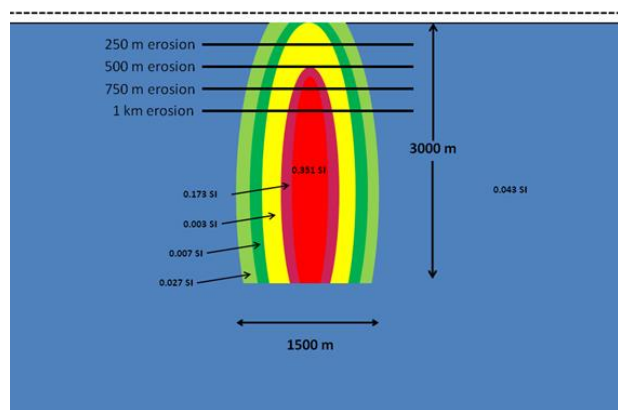


Figure 3. Alteration zonation model of a gold-rich porphyry copper system with maximal development of a biotite-magnetite assemblage in the potassic zone. There is no vertical exaggeration. Intense potassic alteration in the core of the deposit is shown in bright red, the surrounding shells of less intense potassic, phyllic, intense propylitic and moderate propylitic alteration are shown in purple, yellow, dark green and light green respectively. The host rock shown in blue represents magnetic mafic-intermediate rocks (nominally andesite) belonging to an oxidized magmatic suite. The location of the calculated magnetic profile over the uneroded deposit is indicated by the dashed black line. The black horizontal lines indicate exposure level of the system after removal of 250, 500, 750 and 1000 m by erosion.

Figure 5 shows magnetic profiles over an uneroded gold-rich porphyry copper model with a typical development of a biotite-magnetite assemblage in the potassic alteration zone, for differing host rocks and erosion levels. For magnetic mafic-intermediate igneous host rocks (represented by andesite in Figure 3) the signature of the uneroded deposit is a magnetic low, reflecting the negative magnetization contrast between the large volume of the magnetite-destructive phyllic and propylitic zones and the surrounding magnetic unaltered rocks. As deeper levels of the system are exposed the signature gains a central high within an annular low. For weakly magnetic felsic host rocks the effects of magnetite-destructive alteration are less important and the signature for an eroded system is a broad high, reflecting the deeply buried magnetic potassic core of the system. For an uneroded system hosted by felsic rocks the signature is very weak (amplitude 31 nT), as the most significant magnetization contrast corresponds to the deeply buried potassic core, which has lower magnetization than the corresponding zone in Figure 3.

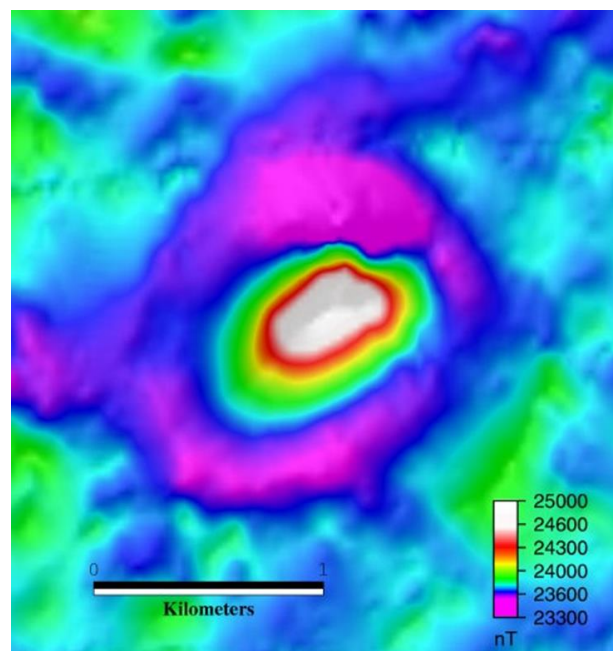


Figure 4. RTP magnetic anomaly pattern over the Bajo de la Alumbrera Cu-Au porphyry deposit, Catamarca Province, Argentina, hosted by magnetic andesitic volcanics of the Farallon Negro Formation. The central magnetic high is due to the potassic (biotite-magnetite) core zone and the annular magnetic low is due to magnetite destruction within the surrounding phyllic zone. In the outer propylitic zone the magnetic response gradually returns to the background level and to the busy texture associated with the andesitic host rocks.

These models have been extended to include other geological settings, including emplacement into different host rocks, or along a contact between contrasting lithologies, post-emplacment tilting and faulting of deposits, different erosion levels, and burial by younger overburden, all of which affect the predicted signature (Clark *et al.*, 2004; Clark, 2014). Models of other types

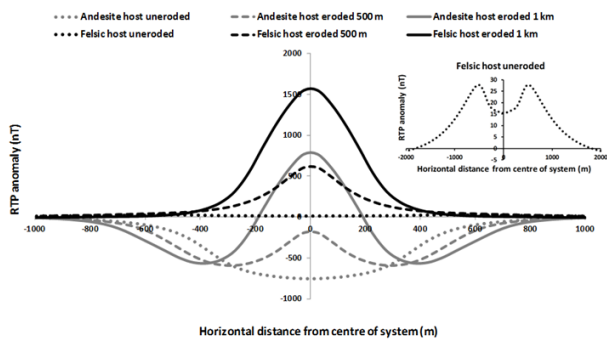


Figure 5. Theoretical RTP magnetic profiles over a gold-rich porphyry copper model with a typical development of a biotite-magnetite assemblage in the potassic alteration zone, for differing host rocks and erosion levels. Profiles were calculated as described in Figure 3. The inset shows the low amplitude (30 nT) signature of the uneroded system in felsic host rocks, which is not clearly visible at the scale of the main plot.

of porphyry copper and epithermal gold deposit that have been developed include high- and low-sulfur variants of the Lowell and Guilbert (1970) quartz-monzonite model, models of Chilean giant porphyry copper deposits with supergene blankets, reduced porphyry models, and high- and low-sulfidation volcanic-hosted epithermal gold deposits.

IOCG models

Clark *et al.*, (2004) developed a suite of predictive magnetic exploration models for IOCG deposits, some of which have been presented in Clark (2014). In a typical vertically zoned IOCG system, magnetite-destructive, hematite-rich HSCC alteration dominates upper levels, whereas magnetite-rich alteration dominates at depth. Thus the current erosion level determines whether the exposed or near-surface portions of the system are hematite-rich or magnetite-rich. Magnetite is also abundant peripheral to the upper hematite-rich zones.

The general zoning pattern inferred for IOCG deposits is shown in Figure 6 and Table 6 lists the characteristic mineralogy of the alteration zones. Magnetic properties of the zones are listed in Table 7. This pattern may be altered by tectonic tilting of the system or by faulting. Therefore the magnetic and gravity signatures of IOCG deposits should generally reflect *superposed* or *juxtaposed* gravity and magnetic anomalies. Positive gravity anomalies arise from both magnetite-rich and hematite-rich zones, whereas the deeper, peripheral, or adjacent magnetic sources correspond to the magnetite-rich zones.

Figure 7 shows images and contour maps of predicted RTP signatures of IOCG systems. Uneroded systems produce substantial magnetic anomalies whether developed within mafic or felsic host rocks, due to high concentrations of iron oxides, associated with strong Fe metasomatism, over large volumes. Magnetic signatures are predicted to be stronger for more mafic systems and amplitudes also increase substantially if deeper levels of the system are exposed by erosion. Up-

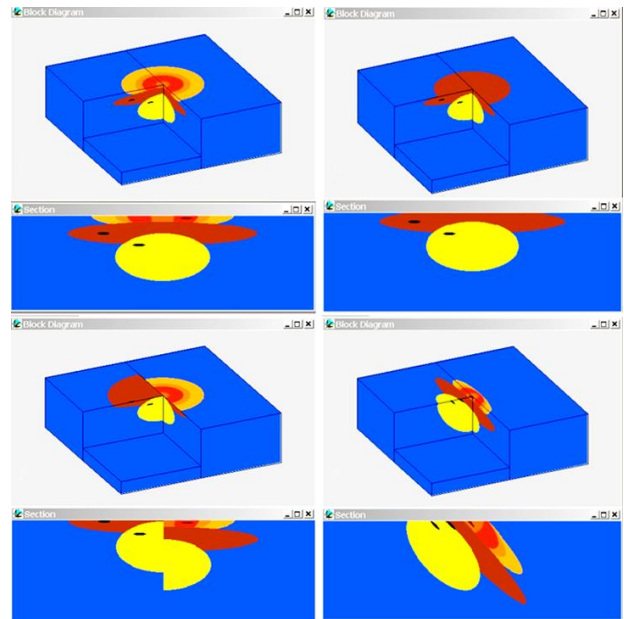


Figure 6. IOCG models hosted by an oxidized mafic lithology (blue). Dimensions of the block models are 12.8 km × 12.8 km × 4 km. The other zones are: outer hematite halo (yellow), inner hematite halo (orange), hematite breccia (red), quartz-hematite core (light brown), potassic alteration (mid brown), massive hematite (dark brown), deep sodic alteration (lemon yellow), discrete massive magnetite bodies (black). Top left: uneroded system; top right: after 400 m removed by erosion; bottom left: after vertical dip-slip fault has juxtaposed magnetite- and hematite-rich portions of system; bottom right: after tilting of system through 45°.

faulting of the magnetite-rich deeper portion of the system (Figure 6, bottom left) results in strong signatures over this segment of the system, juxtaposed with more subdued anomalies over the hematite-rich segment. This scenario is analogous to the Prominent Hill, South Australia IOCG deposit, where the Cu-Au mineralization occurs within a weakly magnetic massive hematite zone that is outlined by a gravity high, separated by a fault from the strongly magnetic and dense magnetite-rich zone that represents an originally deeper portion of the system, prior to faulting (Belperio *et al.*, 2007). Juxtaposed hematite-rich and magnetite-rich segments of an IOCG system can also result from tectonic tilting (Figure 6, bottom right) with a predicted signature shown in Figure 7 (bottom right).

The predictive models provide insights into the highly variable magnetic signatures of known IOCG deposits, their varying relationships to the associated gravity anomalies, and the dependence of the potential field signatures on the geological history of each deposit. Overall the magnetic sources of anomalies associated with IOCG deposits tend to be deeper and more laterally extensive than the gravity sources.

CONCLUSIONS – EXPLORATION CRITERIA

AMIRA International project P700 developed exploration criteria for porphyry, epithermal and IOCG deposits, based on petrophysical and geophysical case studies and on insights gained

from model studies (Clark *et al.*, 2004). These exploration guidelines are summarized below.

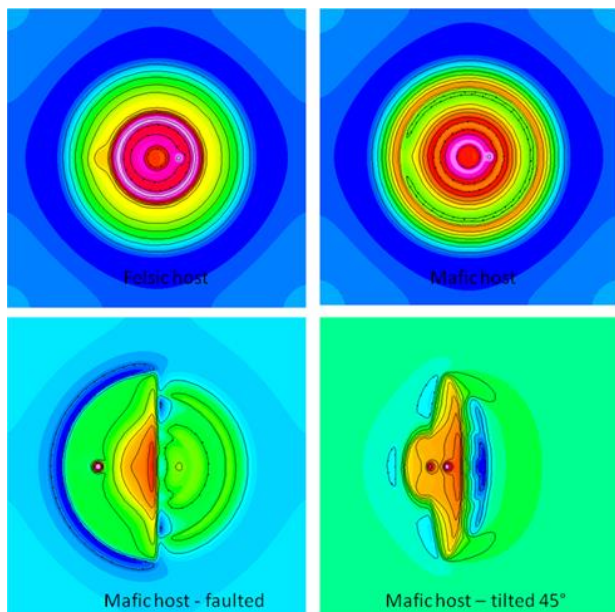


Figure 7. Predicted magnetic signatures of IOCG systems depicted in Figure 6. Top left: uneroded system hosted by moderately magnetic oxidized felsic rocks (contour interval 200 nT); top right: uneroded system hosted by oxidized magnetic mafic rocks (contour interval 200 nT); bottom left: faulted system hosted within mafic rocks (contour interval 600 nT); system hosted by mafic rocks, tilted 45° (contour interval 500 nT). Dimensions of the magnetic images are 12.8 km × 12.8 km.

Indicators of tectonic setting

- In areas of extensive cover, regional potential field data sets, supplemented by seismic, magnetotelluric or other deep-penetrating methods, may be useful for delineating favorable geological environments for ore deposits of particular types.
- Subduction-related magmatic arcs are favorable settings for porphyry, epithermal and some, generally younger, IOCG deposits. These areas are characterized by linear parallel belts of gravity and magnetic highs and lows.
- Magnetic high zones correspond to belts of magnetite-series granitoids and are most favourable for porphyry Cu, Cu-Au, and Cu-Mo deposits, HS and LS epithermal deposits and IOCG deposits.
- Magnetic low belts may correspond to sedimentary basins (e.g. back arc basins), which can be recognized from their gravity lows, or to belts of reduced, ilmenite-series granitoids, which are prospective for Sn and also for intrusive-related Au and reduced porphyry Au-(Cu) deposits.

- Anorogenic settings, e.g. failed continental rifts and passive Atlantic-type continental margins, are favourable for IOCG deposits, particularly of Precambrian age. Buried terrains with this character may be recognizable from linear rift-parallel regional gravity and magnetic highs along the ancient continental margin, with a quiet magnetic zone outboard of the regional highs and relatively busy magnetic patterns inboard of the margin.
- Bimodal magmatism associated with anorogenic settings is characterized by contrasting highly magnetic and weakly magnetic intrusions, which are often evident in regional magnetic and gravity data.

Indicators of favourable structures

- At a regional scale major structures that control the emplacement of mineralizing or heat-engine magmas, or channel flow of crustal fluids, are often evident in suitably processed gravity and magnetic data sets. These features may also be visible in satellite imagery. Intersections of lineaments appear to be particularly favourable for IOCG mineralization.
- Structural controls at a range of scales, from province to prospect scale, may be evident in detailed magnetic data. Intersections of such lineaments appear to be favourable for porphyry and/or epithermal mineralization.
- Identification of favourable orientations of structures may be possible if senses of movement, block rotations etc. are known. Anomaly offsets and abrupt changes of trend in magnetic images can help to define tectonic movements. Paleomagnetic studies can also be useful for defining rotations and tilting within and around deposits.

Indicators of fractional crystallisation

- At a semi-regional scale, zoned plutons, with correspondingly zoned magnetic properties, densities and radioelement concentrations, are indicative of fractional crystallisation and suggest potential for development of magmatic-hydrothermal systems.
- Multiple/nested intrusions, with a substantial range of magnetic properties, densities and radioelement contents, particularly when there are geophysical indications of an underlying magma chamber, are also favourable indicators of fractional crystallisation.
- Well-developed contact aureoles are indicative of emplacement of high-temperature, melt-rich magma capable of undergoing substantial fractional crystallization.
- Strong contact aureole effects produce substantial mineralogical changes in the metamorphosed and metasomatized host rocks, often with pronounced changes in magnetic susceptibility (particularly increased susceptibility due to creation of secondary magnetite and/or pyrrhotite).

- Strong remanent magnetization of contact aureoles is diagnostic of high temperature emplacement or substantial metasomatism.

Understanding effects of primary composition and alteration on magnetic properties

- Understanding the effects of protolith composition and alteration type on magnetic properties is crucial for evaluating magnetic signatures of hydrothermal systems. Cu-Au is associated with more magnetic magmatic-hydrothermal systems than Cu-Mo; W-Mo-Bi and Au in tin provinces is much less magnetic. In oxidized Au-bearing systems, Au mineralization is often associated with the felsic end of magmatic evolution and is then associated locally with a weaker magnetic character and higher radioelement contents.
- Strong alteration zoning of magnetic character is favourable: early potassic alteration, particularly of mafic protoliths, is often magnetite-rich, contrasting strongly with phyllic overprinting, which is magnetite-destructive. Large zones of contrasting intense alteration suggest development and preservation of a mature hydrothermal system.

Superposed or Juxtaposed Gravity and Magnetic Anomalies

- Iron oxide copper-gold deposits occur within Fe-metasomatic systems that are typically zoned from magnetite-dominant to hematite-dominant.
- The primary zonation is usually from magnetite-dominant at depth to hematite-dominant at shallower levels, producing magnetic and gravity highs that are *superposed* not simply *coincident*, i.e. detailed analysis of the anomalies should reveal that the magnetic source is deeper than the gravity source.
- Tilting or faulting of an IOCG deposit may juxtapose the magnetite-dominant and hematite-dominant zones, producing *juxtaposed* gravity and magnetic anomalies
- Even without tilting or faulting, magnetite-enhanced alteration often occurs peripheral to hematite-dominant systems. This again will produce juxtaposed, rather than coincident, magnetic and gravity anomalies.
- Hematite-rich deposits that have undergone high-grade metamorphism to greater than ~650°C can be expected to carry intense remanence, with a strong magnetic anomaly. Either regional metamorphism to upper amphibolite-granulite grade or contact metamorphism due to a nearby intrusion could produce this effect. The form of the anomaly may be diagnostic of strong remanence, if the paleofield recorded is oblique to the present field – which is very likely if the magnetization is ancient.

Use of predictive models to prioritise targets

- The predictive exploration models can assist recognition of deposit signatures that are appropriate for the local geological setting. Predicted signatures vary greatly depending on the deposit type, the host rocks, post-formation faulting or tilting and so on.
- Predictive models can also be used to assess the detectability of particular types of deposit in the local geological setting. For example, an intact gold-rich porphyry copper deposit buried beneath 100 m of magnetic volcanics should be detectable in most cases, whereas a typical giant porphyry copper of the Chilean Andes would be difficult to detect beneath such cover, although it should be visible beneath sedimentary overburden, provided it is emplaced into fairly magnetic rocks.
- The observed signatures depend not only on the local geological environment, but on local to semi-regional geomagnetic field gradients, which can distort the signatures substantially. Calculated grids generated for each model can be used to study the effects of geomagnetic field distortion and aid recognition of distorted signatures.

Other considerations

- Although magnetics can be a very useful tool for locating prospective hydrothermal systems, location of ore zones within the system often requires alternative methods. Electrical and, in some cases, electromagnetic methods, are generally more sensitive to sulfide-rich mineralization.
- An empirical tendency for remanent magnetic signatures to be more common in mineralized intrusive systems than barren systems is suggested by case studies.
- Subtle alteration zoning of magnetic mineralogy may be detectable paleomagnetically. For example the host rocks to the Mount Leyshon Au deposit in Queensland carry syn-mineralization overprints that are detectable well beyond the zone of visible alteration and are zoned from proximal magnetite to distal hematite (Clark and Lackie, 2003).

REFERENCES

- Airo, M. L., 2002, Aeromagnetic and aeroradiometric response to hydrothermal alteration: Surveys in Geophysics, 23(4), 273-302.
- Allis, R.G., 1990, Geophysical anomalies over epithermal systems: Journal of Geochemical Exploration, 36, 339-374.
- Belperio, A., Flint, R., Freeman, H., 2007, Prominent Hill: A Hematite-Dominated, Iron Oxide Copper-Gold System: Economic Geology, 102, 1499-1510.
- Beane, R.E., 1994, A graphic view of hydrothermal mineral stability relations, in: D.R. Lentz, ed., Alteration and Alteration

Processes Associated with Ore-forming Systems: Geological Association of Canada Short Course Notes, 11, 1-30.

Blevin, P.L., Chappell, B.W., 1992, The role of magma sources, oxidation states and fractionation in determining the granite metallogeny of eastern Australia: Transactions of the Royal Society of Edinburgh, Earth Sciences, 83, 305-316.

Champion, D.C., Heinemann, M.A., 1994, Igneous rocks of northern Queensland: 1:500,000 map and GIS explanatory notes: AGSO Record 1994/11.

Clark, A.H. and Arancibia, O.N., 1995, The occurrence, paragenesis and implications of magnetite-rich alteration-mineralization in calc-alkaline porphyry copper deposits., in A.H. Clark, ed., Giant Ore Deposits - II, Controls on the Scale of Orogenic Magmatic-Hydrothermal Mineralization: Proceedings of the Second Giant Ore Deposits Workshop, Kingston, Ontario, Canada, April 25-27, 1995, 583-640.

Clark, D.A., 1988, Catalogue of magnetic properties of Australasian rocks III: CSIRO Division of Exploration Geoscience, Restricted Investigation Report 1746R.

Clark, D.A., 1997, Magnetic petrophysics and magnetic petrology: aids to geological interpretation of magnetic surveys: AGSO Journal of Australian Geology and Geophysics, 17, 83-103.

Clark, D.A., 1999, Magnetic petrology of igneous intrusions: implications for exploration and magnetic interpretation: Exploration Geophysics, 30, 5-26.

Clark, D.A., 2014, Magnetic effects of hydrothermal alteration in porphyry copper and iron-oxide copper-gold systems: A review: Tectonophysics, 624-625, 46-65.
<http://dx.doi.org/10.1016/j.tecto.2013.12.011>

Clark, D.A., French, D.H., Lackie, M.A., Schmidt, P.W., 1992, Magnetic petrology: application of integrated rock magnetic and petrological techniques to geological interpretation of magnetic surveys: Exploration Geophysics, 23, 65-68.

Clark, D.A., Geuna, S.E., Schmidt, P.W., 2004, Predictive magnetic exploration models for porphyry, epithermal and iron oxide Cu-Au deposits: P700 Final Report, AMIRA International.
<https://confluence.csiro.au/display/cmfr/Historic+Publications?preview=/26574957/26575544/Clark%20etal%202004%20P700%20CSIRO%201073Rs.pdf>

Clark, D.A. and Lackie, M.A., 2003, Palaeomagnetism of the Early Permian Mount Leyshon Intrusive Complex and Tuckers Igneous Complex, North Queensland, Australia: Geophysical Journal International, 153, 523-547.

Criss, R.E., Champion, D.E., 1984, Magnetic properties of rocks from the southern half of the Idaho Batholith: influences of hydrothermal alteration and implications for aeromagnetic interpretation: Journal of Geophysical Research, 89, 7061-7076.

Criss, R.E., Champion, D.E. and McIntyre, D.H., 1985, Oxygen isotope, aeromagnetic, and gravity anomalies associated with hydrothermally altered zones in the Yankee Fork mining district, Custer County, Idaho: Economic Geology, 80, 1277-1296.

Einaudi, M.T., 1982, Description of skarns associated with porphyry copper plutons: southwestern North America, in S.R. Titley, ed., Advances in Geology of the Porphyry Copper Deposits, Southwestern North America: University of Arizona Press, Tucson, 139-183.

Einaudi, M.T., Meinert, L.D. and Newberry, R.J., 1981, Skarn deposits: Economic Geology, 75th Anniversary Volume, 317-391.

Finn, C.A., Sisson, T.W., Deszcz-Pan, M., 2001, Aerogeophysical measurements of collapse-prone hydrothermally altered zones at Mount Rainier volcano: Nature, 409, 600-603.

Finn, C.A., Morgan, L.A., 2002, High-resolution aeromagnetic mapping of volcanic terrain, Yellowstone National Park: Journal of Volcanology and Geothermal Research, 115, 207-231.

Finn, C.A., Deszcz-Pan, M., Anderson, E.D., John, D.A., 2007, Three-dimensional geophysical mapping of rock alteration and water content at Mount Adams, Washington: Implications for lahar hazards: Journal of Geophysical Research, 112, B10204.

Irvine, R.J., Smith, M.J., 1990, Geophysical exploration for epithermal gold systems: Journal of Geochemical Exploration, 36, 375-412.

Ishihara, S., 1981, The granitoid series and mineralization: Economic Geology, 75th Anniversary Volume, 458-484.

Ishihara, S., Sawata, H., Arpornsuwan, S., Busaracome, P., Bungbrakearti, N., 1979, The magnetite-series and ilmenite-series granitoids and their bearing on tin mineralization, particularly of the Malay Peninsula region: Geological Society of Malaysia. Bulletin 11, 103-110.

Lapointe, P., Morris, W.A., Harding, K.L., 1986, Interpretation of magnetic susceptibility: a new approach to geophysical evaluation of the degree of rock alteration: Canadian Journal of Earth Sciences, 23(3), 393-401.

Lowell, J.D., Guilbert, J.M., 1970, Lateral and vertical alteration-mineralization zoning in porphyry copper deposits: Economic Geology, 65, 373-408.

Purucker, M., Clark, D.A., 2011, Mapping and interpretation of the lithospheric magnetic field, in M. Mandea, M. and M. Korte, eds., Geomagnetic Observations and Models: IAGA Special Sopron Book Series 5, Springer, 311-337.

Sillitoe, R.H., 1979, Some thoughts on gold-rich porphyry copper deposits: Mineralium Deposita, 14, 161-1744.

Sillitoe, R.H., 1990, Gold-rich porphyry copper deposits of the circum-Pacific region - an updated overview: Pacific Rim 90 Congress Proceedings, 119-126.

Sillitoe, R.H., 1993, Gold-rich porphyry copper deposits: geological model and exploration implications, in B.H. Whiting, R. Mason and C.J. Hodgson, eds., Giant Ore Deposits: Society of Economic Geologists, Special Publication 2, 305-362.

Sillitoe, R.H., 1996, Characteristics and controls of the largest porphyry copper-gold and epithermal gold deposits in the circum-Pacific region: Australian Journal of Earth Sciences, 44, 373-388.

Studemeister, P.A., 1983, The redox state of iron: a powerful indicator of hydrothermal alteration: Geoscience Canada, 10, 189-194.

Webster, S.S., 1984, A magnetic signature for tin deposits in south-east Australia: Exploration Geophysics, 15, 15-31.

Wyborn, L.A. and Heinrich, C., 1993a, The relationship between late-tectonic felsic intrusives and Cu-Au mineralisation in the Eastern Fold Belt, Mount Isa Inlier, in Symposium on Recent Advances in the Mount Isa Block, Australian Institute of Geoscientists Bulletin, 13, 27-30.

Wyborn, L.A. and Heinrich, C., 1993b, Empirical observations on granite-associated gold \pm base-metal mineral deposits in the Proterozoic of Australia: AGSO Research Newsletter, 19, 3-4.

Wyborn, L. and Stuart-Smith, P., 1993, The relationship between granite composition, host rock types, and Au \pm base-metal mineralisation in the Cullen Mineral Field, Pine Creek Inlier: AGSO Research Newsletter, 19, 5-8.

Table 4. Porphyry copper deposits: equivalent alteration stages/differing host rocks (Beane, 1994)

Stage	Quartz Monzonite	Diorite	Limestone
Early	K-feldspar + biotite + pyrite + magnetite or hematite	Biotite + KF + albite + epidote + magnetite	Garnet + pyroxene
Copper mineralization	KF + chlorite + sericite + pyrite ± hematite	Chlorite + epidote + pyrite + magnetite	Actinolite + epidote + pyrite + magnetite
Late	Sericite + pyrite	Chlorite + anhydrite + pyrite + hematite + ?zeolite	Quartz + pyrite

Table 1. Characteristic Mineral Assemblages of the Main Alteration Types in Porphyry Systems and Associated Magnetic Properties

ALTERATION TYPE (synonym)	CHARACTERISTIC ASSEMBLAGE [magnetic effects]
Early magnetite \pm amphibole \pm plagioclase veins (M veins)	Quartz-magnetite \pm amphibole \pm plagioclase, sulfide-poor veins; Fe-metasomatism (Clark and Arancibia, 1995) [abundant multidomain magnetite created: high k , $Q < 1$]
Potassic (K-silicate)	K-feldspar and/or biotite, plus one or more of: sericite, chlorite and quartz (e.g. in the interior zone of porphyry copper deposits) [Usually magnetite-producing (increased k , $Q < 1$): up to 5 vol % in mafic/intermediate rocks (e.g. gold-rich porphyry copper deposits); minor magnetite addition in felsic rocks; often associated with early quartz-magnetite-(amphibole) veins. Sometimes magnetite-destructive in high sulfidation systems.]
Phyllic (Sericitic)	Quartz-sericite-pyrite-chlorite (e.g. in large halos around porphyry copper deposits) [Magnetite-destructive (pyrite + hematite produced); decreased k]
Intermediate Argillic	Smectite and kaolinite, commonly replacing plagioclase (e.g. variably developed zone outside sericitic zone in some porphyry coppers) [magnetite-destructive; decreased k]
Propylitic	Albite (or K-feldspar in potassic rocks), chlorite and epidote group minerals; with only minor change in bulk composition (e.g. outermost alteration zone of porphyry copper deposits) [strong: Partially to totally magnetite-destructive (Fe in pyrite, hematite, epidote, chlorite, actinolite), decreased k] [weak: magnetite stable, k unchanged]
Albitic	Na-rich plagioclase + epidote and other propylitic minerals; with substantial addition of Na [magnetite-destructive, decreased k]
Sodic-calcic	Sodic feldspar and epidote \pm actinolite \pm chlorite (e.g. adjacent to intrusion at depth, beneath certain porphyry copper deposits) [magnetite-destructive, decreased k]
Advanced Argillic	Quartz plus one or more of: kaolinite, dickite, pyrophyllite, diaspore, pyrite, alunite, zunyite, topaz (e.g. in epithermal systems that may overlie porphyry systems) [magnetite-destructive, decreased k]
Carbonate	Calcite, dolomite, ankerite, siderite plus sericite, pyrite and/or albite [partially magnetite-destructive, decreased k]
Skarn	Ca and Mg silicates (limestone protolith: andradite and grossular, wollastonite, epidote, idocrase, chlorite, actinolite; dolostone protolith: forsterite, serpentine, talc, brucite, tremolite, chlorite) [see Tables 3 and 4]
Supergene oxidation	Alunite, allophane, jarosite, Fe oxides, sulfates [magnetite- and pyrrhotite-destructive; hematite and goethite produced; decreased k]

Table 2. Typical magnetic properties of skarns

LITHOLOGY	Av. $k \pm SE$ (10^{-3} SI) [Range]	ΔB_z (nT)*	Average NRM $\pm SE$ [Range] (A/m) Average $Q \pm SE$ [Range]
Oxidized Magnetite Skarn†	650 ± 160 [120 - 2000]	$16,250 \pm 4000$ [3000 - 50,000]	$J = 50 \pm 20$ [0.3 – 210] $Q = 1.4 \pm 0.4$ [0.05 – 4.5]
Reduced Pyrrhotite Skarn†	5 ± 2 [1 - 8]	125 ± 50 [25 – 200]	$J = 14 \pm 8$ [1 – 34] $Q = 16 \pm 4$ [8 – 25]
Reduced pyroxene \pm garnet† skarn (mt rare or absent)	1.1 ± 0.2 [0.1 - 2]	28 ± 5 [2.5 – 50]	$J < 0.02$ $Q \ll 1$
Calcic Fe (Cu, Co, Au) skarn‡ (mafic intrusion; island arc or rifted continental margin)	2000 [1200 - 3500]	50,000 [30,000 – 175,000]	J : [5 – 300] $Q \sim 1$ [0.1 – 5]
Magnesian Fe (Cu, Zn) skarn‡ (felsic intrusion; continental margin)	2000 [1200 – 2700]	100,000 [60,000 – 87,500]	J : [5 – 220] $Q \sim 1$ [0.1 – 5]
Calcic Cu (Mo, W, Zn) skarn - proximal‡ (Grd-Qmz; continental margin)	[30 - 400]	[750 – 10,000]	J : [1 – 50] $Q \sim 1.5$ [0.1 – 5]
Magnesian Cu (Mo, W, Zn) skarn‡ (Grd-Qmz; continental margin)	[800 -1700]	[20,000 – 42,500]	J : [5 – 100] $Q \sim 1.5$ [0.1 – 5]

* ΔB_z is the maximum associated magnetic anomaly (steep field, non-magnetic country rocks, diameter \gg depth below sensor, great depth extent), calculated from total magnetization for case where remanence is parallel to induced magnetization. The effective susceptibility is therefore taken to be $k(1+Q)$. †Averages from P700 Database and from CSIRO Catalogue of Magnetic Properties (Clark, 1988). ‡Inferred values from data in Einaudi et al. (1981).

Table 3. Zonation of mineralogy and magnetic properties of a typical copper skarn (deep skarn, Carr Fork mine, Bingham Mining District, Utah)

ZONE	Distance from intrusive contact (m)	GANGUE	SULFIDES	Cu (wt %)	Magnetite (vol %)	k* (10⁻³ SI)
Bingham stock (potassic zone)	> 100	qtz, Kfsp, bio	cp, bn, py	0.65 (shallow) < 0.1 (deep)	0.1 –1	3.5 – 35
Endoskarn (Bingham stock)	< 100	act, ep	(0.5 vol %) mb > cp	< 0.1	~ 0.1	~ 3.5
Proximal exoskarn	0-50	and > di, cal, qtz,	(1-2 vol %) cp, (bn)	~0.2	1-2	35 - 70
Exoskarn	50 – 100	and	(2-5 vol %) cp > py	~ 0.6	2 - 5	70 - 180
Exoskarn	100 – 300	and >> di	(15 vol %) cp ≥ py	~ 8	5 – 10	180 - 380
Exoskarn	300 - 350	and ≥ di	(5 vol %) cp:py = 0.2	~ 0.5	2	70
Exoskarn	350 – 400	wo (gar, di)	(1 vol %) bn, cp, sph, (py)	~ 0.5	< 0.1	< 3.5
Distal exoskarn	400 - 600	wo-di-qtz; marble	wo-cal; (0.5 vol %) bn, cp, sph, gal	< 0.5	< 0.1	< 3.5
Marble, limestone	> 600	cal, marble	(< 0.1 vol %) (sph, gal, py)	0	0	0

Ore zone (~120-600 m from contact) average grades: ~2.3 % Cu, 0.6 g/t Au, 12 g/t Ag, 0.03 % Mo.

Mineralogical and chemical data from Einaudi (1982).

*Susceptibilities calculated using equation (3) from petrographically estimated modal magnetite contents.

Table 5. Dimensions and susceptibilities of zones comprising the gold-rich porphyry copper model with maximal development of a magnetite-rich potassic core

Zone	Diameter* (m)	Width* (m)	Depth extent (m)	Susceptibility (SI)
Inner potassic	360	360	2400	0.351
Outer potassic	600	120	2500	0.173
Phyllic	1000	200	3000	0.003
Strong propylitic	1200	100	3000	0.007
Weak propylitic	1500	150	3000	0.027
Andesite/Basalt/ Diorite/Gabbro	Very large	Very large	3000	0.043

* Diameters and widths of zones are maxima (at a depth 2000 m below the top of the phyllic zone for the propylitic and phyllic zones, and 1000 m below the top of the phyllic zone for the potassic zones).

Table 6. Characteristic Mineral Assemblages of the Main Alteration Types in IOCG Systems

ALTERATION TYPE (synonym)	CHARACTERISTIC ASSEMBLAGE [magnetic effects]
Sodic	extensive albitisation of host rocks, accompanied by magnetite ± scapolite ± chlorite ± actinolite ± hematite [abundant multidomain magnetite created: high k , $Q < 1$]
Sodic-calcic	plagioclase-magnetite-epidote-calcite-sphene ± scapolite ± chlorite ± actinolite ± garnet ± hematite [abundant multidomain magnetite created: high k , $Q < 1$]
Sodic-potassic	albite-K feldspar-magnetite-quartz ± sericite ± biotite ± hematite ± chlorite ± actinolite [abundant multidomain magnetite created: high k , $Q < 1$]
Potassic-calcic	K feldspar-biotite-magnetite-epidote-calcite-sphene ± chlorite ± actinolite ± garnet ± hematite [abundant multidomain magnetite created: high k , $Q < 1$]
Potassic	K feldspar-sericite-magnetite-quartz ± biotite ± hematite ± chlorite ± actinolite [abundant multidomain magnetite created: high k , $Q < 1$]
Sericite-hematite (HSCC, argillic, hydrolytic)	sericite-hematite-chlorite-carbonate ± quartz [abundant multidomain hematite created: low k ; $Q < 1$, unless high-grade metamorphosed]

Table 7. Typical magnetic properties and densities of IOCG-style alteration systems (low metamorphic grade)

ZONE	Vol. % magnetite	Vol. % hematite	Calculated susceptibility* (10^{-3} SI)	Calculated Density (kg/m^3)
Felsic Host	0.15	0	5.2	2650
Outer hematite halo - upper (HSCC) zone	0.2	2	7.7	2710
Inner hematite halo - upper (HSCC) zone	2	4	72	2800
Hematite breccia - upper (HSCC) zone	1	36	49	3590
Hematite-quartz breccia - upper (HSCC) zone	0	37	15	3590
Massive hematite lens	0	60	24	4180
Potassic/Potassic-calcic/sodic/sodic-calcic deep zones	3.5	0	124	2740
Massive magnetite lens	60	0	4110	4180
Mt-rich Mafic Host	5.2	0	187	3000
Outer hematite halo - upper (HSCC) zone	2	5	72	3040
Inner hematite halo - upper (HSCC) zone	2	9	74	3140
Hematite breccia - upper (HSCC) zone	1	41	51	3810 ($\rho_G = 2800$)
Hematite-quartz breccia - upper (HSCC) zone	0	42	17	3810 ($\rho_G = 2800$)
Massive hematite lens	0	60	24	4240 ($\rho_G = 2800$)
Potassic/Potassic-calcic/sodic/sodic-calcic deep zones	8.5	0	315	3080
Massive magnetite lens	60	0	4110	4270

* Susceptibility calculated from magnetite and hematite contents, using equation (3).

ρ_G = assumed gangue density (2650 kg/m^3 for felsic host; 2880 kg/m^3 for mafic host, except where sericitic alteration is dominant). Density is calculated as

$\rho = \rho_{\text{GANGUE}} + (\rho_{\text{OXIDES}} - \rho_{\text{GANGUE}})(f_{\text{MT}} + f_{\text{HM}})$, where $\rho_{\text{OXIDES}} = 5200 \text{ kg/m}^3$.